

$\rho^0 \Delta^{++}$ and $\omega \Delta^{++}$ Joint Decay Correlations at 3.7 GeV/c*K. W. J. Barnham,[†] G. S. Abrams, W. R. Butler,[‡]G. Goldhaber,[§] B. H. Hall, and J. MacNaughton^{||}*Department of Physics and Lawrence Berkeley Laboratory, University of California, Berkeley, California 94720*

(Received 14 September 1972)

The joint decay density-matrix elements have been measured for the $\rho^0 \Delta^{++}$ and $\omega \Delta^{++}$ channels at 3.7 GeV/c. The data are presented as a function of momentum transfer in both the t -channel and s -channel coordinate systems. The presence of correlated decays is illustrated for both reactions by employing selective cuts on the decay angles of one resonance, and displaying the effects on the decay distribution of the opposing resonance. An amplitude analysis is performed with the data near 0° production angle, where we obtain a helicity decomposition of the scattering amplitude with no experimental ambiguity.

I. INTRODUCTION

The utility of decay angular distributions of resonances in the study of production dynamics has long been recognized.¹ For peripheral processes the decay density-matrix elements give insights into the role of particle exchanges that cannot be obtained from studies of the differential cross sections alone. The double-resonance-production reactions $\pi N \rightarrow \rho \Delta$ and $\pi N \rightarrow \omega \Delta$, in particular, are well suited for such a study since analysis of the decay of each final-state particle is possible. Partial results from this experiment have been previously reported² for these reactions, with an emphasis on enumerating the dominant exchange processes as revealed by a study of single-vertex decay density-matrix elements.

For a detailed study of production mechanisms, however, the extraction of production amplitudes from the data is desirable. Just as information is lost if one sums over spin states to investigate differential cross sections, so too is information lost if one neglects possible correlations in the decay angular distributions of the vector meson with the isobar.

In this paper we present our data for all of the measurable parameters for $\pi^+ p \rightarrow \rho^0 \Delta^{++}$ and $\omega \Delta^{++}$ (for an unpolarized target and for an unobserved final-state nucleon polarization). The data are presented in the t -channel coordinate system,¹ since peripheral dynamics is most conveniently expressed in this frame. For completeness, however, we also present the data in the s -channel (helicity) coordinate system.

We show that several correlation terms are significant for each reaction studied. Earlier experiments^{3,4} have noted the presence of these terms for at least one of the reactions $\rho \Delta$ and $\omega \Delta$. With increased statistics we are able to study the mo-

mentum-transfer dependence of the decay correlations. We are also able to exhibit the correlations visually, so that the content of the correlations insofar as they affect the joint decay angular distribution becomes apparent. Finally, it is shown that the constraints of angular momentum conservation are sufficiently severe at 0° production angle⁵ that some of the production amplitudes may be calculated directly from the data.

A comparison of the data with the constraints of the nonrelativistic quark model will be presented in another paper.⁶

II. EXPERIMENTAL METHOD

The data were obtained from a 200 000-picture exposure of the Lawrence Berkeley Laboratory 72-in. hydrogen bubble chamber to a π^+ beam of central momentum 3.7 GeV/c at the Bevatron. Using standard reconstruction, kinematic fitting, and event-selection techniques, we have obtained the following numbers of events in the final states of interest to this study:

$$\pi^+ p \rightarrow p \pi^+ \pi^+ \pi^- \quad 16\,445 \text{ events}, \quad (1)$$

$$\pi^+ p \rightarrow p \pi^+ \pi^+ \pi^- \pi^0 \quad 16\,617 \text{ events}. \quad (2)$$

The quasi-two-body channels $\rho^0 \Delta^{++}$ and $\omega \Delta^{++}$ were selected from the final states (1) and (2), respectively, via the following mass-band criteria.

$$\rho^0: 680 \text{ MeV}/c^2 \leq M(\pi^+ \pi^-) \leq 860 \text{ MeV}/c^2,$$

$$\omega: 763 \text{ MeV}/c^2 \leq M(\pi^+ \pi^- \pi^0) \leq 803 \text{ MeV}/c^2,$$

$$\Delta^{++}: 1160 \text{ MeV}/c^2 \leq M(p \pi^+) \leq 1280 \text{ MeV}/c^2.$$

The presence of two π^+ mesons in the final states (1) and (2) allows some events (1% for $\rho \Delta$ and much less for $\omega \Delta$) to be counted twice in the data cited below; no significant biases are expected from

such events since their frequency is low. With the above selection criteria the numbers of events for $t' < 1.0$ (GeV/c)² [where $t' \equiv |t - t_{\min}| \approx |t + 0.08|$ (GeV/c)²] are as follows:

$$\pi^+ p \rightarrow \rho^0 \Delta^{++} \quad 3158 \text{ events,} \quad (3)$$

$$\pi^+ p \rightarrow \omega \Delta^{++} \quad 1546 \text{ events.} \quad (4)$$

The coordinate systems used to study the decay distributions of the resonances were conventionally chosen. The quantization (z) axis points along the direction of the incoming particle (beam for ρ^0 or ω decay, and target for Δ^{++} decay), as seen in the rest system of the decaying resonance, in the t -channel (Gottfried-Jackson¹) frame. The z axis for the s -channel (helicity) frame lies along the direction of motion of the decaying system. For both systems the y axis is chosen as the direction of the normal to the production plane, $\vec{p} \times \vec{\Delta}$, while the x axes are chosen so that the systems are

right-handed. The polarization analyzers were chosen as the decay π^+ for $\rho^0 \rightarrow \pi^+ \pi^-$ decay, the decay proton for $\Delta^{++} \rightarrow p \pi^+$, and the normal to the decay plane for $\omega \rightarrow \pi^+ \pi^- \pi^0$.

The general decay distribution for channel (3) or (4) has been given by Pilkuhn and Svensson,⁷ whose notation we adopt. These authors consider the joint decay of a $J^P = 1^-$ and a $J^P = \frac{3}{2}^+$ system, an idealization which is complicated for reaction (3) by the presence of a not-insignificant s -wave $\pi^+ \pi^-$ amplitude (the " ϵ meson"). A standard background subtraction is expected⁸ to correct for this combination if the width of the ϵ is much larger than that of the ρ . For our $\rho \Delta$ data the corrected joint density-matrix elements differed from the uncorrected values by amounts less than the statistical errors for all cases. Hence the effect of the s -wave $\pi^+ \pi^-$ amplitude on the results to be presented below is thought to be small. The Δ^{++} signal for this channel (as well as for $\omega \Delta^{++}$) is contaminated by $\leq 10\%$

TABLE I. General expression for the joint decay angular distribution for $V \Delta$ production, adapted from Ref. 7. We write $W = (1/16\pi^2) [1 + \sum_{i=1}^{19} R_i g_i(\theta_V, \phi_V, \theta_\Delta, \phi_\Delta)]$, with g_i an orthonormal set of functions. The R_i are given below in terms of the ρ_{mm}^{mm} of Ref. 7, and the angular functions h_i are given such that $R_i = \langle h_i \rangle$ (i.e., the proper normalizations for the g_i are provided).

Term	Density-matrix elements ^a	h_i
R_1	$\rho^{0,0}$	$\frac{1}{2} (5 \cos^2 \theta_V - 1)$
R_2	$\text{Re} \rho^{1,0}$	$-(5/4\sqrt{2}) \sin 2\theta_V \cos \phi_V$
R_3	$\rho^{1,-1}$	$-\frac{5}{4} \sin^2 \theta_V \cos 2\phi_V$
R_4	$\rho_{3,3}$	$\frac{1}{8} (7 - 15 \cos^2 \theta_\Delta)$
R_5	$\text{Re} \rho_{3,1}$	$-\frac{5}{8} \sqrt{3} \sin 2\theta_\Delta \cos \phi_\Delta$
R_6	$\text{Re} \rho_{3,-1}$	$-\frac{5}{8} \sqrt{3} \sin^2 \theta_\Delta \cos 2\phi_\Delta$
R_7	$\rho_{3,3} - \rho_{1,1}$	$\frac{25}{8} (1 - 3 \cos^2 \theta_V) (1 - 3 \cos^2 \theta_\Delta)$
R_8	$\rho_{1,-1}$	$-\frac{25}{8} \sin^2 \theta_V \cos 2\phi_V (1 - 3 \cos^2 \theta_\Delta)$
R_9	$\text{Re} \rho_{1,0}$	$\left(\frac{25}{8\sqrt{2}} \right) \sin 2\theta_V \cos \phi_V (1 - 3 \cos^2 \theta_\Delta)$
R_{10}	$\text{Re} \rho_{3,-1}$	$-\frac{25}{16} \sqrt{3} (1 - 3 \cos^2 \theta_V) \sin^2 \theta_\Delta \cos 2\phi_\Delta$
R_{11}	$\text{Re} \rho_{3,1}$	$-\frac{25}{16} \sqrt{3} (1 - 3 \cos^2 \theta_V) \sin 2\theta_\Delta \cos \phi_\Delta$
R_{12}	$\text{Re} \rho_{3,1}^{-1}$	$\frac{25}{32} \sqrt{3} \sin^2 \theta_V \sin^2 \theta_\Delta \cos 2(\phi_V + \phi_\Delta)$
R_{13}	$\text{Re} \rho_{3,1}^{-1,1}$	$\frac{25}{32} \sqrt{3} \sin^2 \theta_V \sin^2 \theta_\Delta \cos 2(\phi_V - \phi_\Delta)$
R_{14}	$\text{Re} \rho_{3,1}^{-1,1}$	$\frac{25}{32} \sqrt{3} \sin^2 \theta_V \sin 2\theta_\Delta \cos(2\phi_V + \phi_\Delta)$
R_{15}	$\text{Re} \rho_{3,1}^{-1,1}$	$\frac{25}{32} \sqrt{3} \sin^2 \theta_V \sin 2\theta_\Delta \cos(2\phi_V - \phi_\Delta)$
R_{16}	$\text{Re}(\rho_{3,-1}^{1,0} - \rho_{3,-1}^{0,-1})$	$\frac{25}{32} \sqrt{6} \sin 2\theta_V \sin^2 \theta_\Delta \cos(\phi_V + 2\phi_\Delta)$
R_{17}	$\text{Re}(\rho_{3,-1}^{0,1} - \rho_{3,-1}^{-1,0})$	$\frac{25}{32} \sqrt{6} \sin 2\theta_V \sin^2 \theta_\Delta \cos(\phi_V - 2\phi_\Delta)$
R_{18}	$\text{Re}(\rho_{3,1}^{1,0} - \rho_{3,1}^{0,-1})$	$\frac{25}{32} \sqrt{6} \sin 2\theta_V \sin 2\theta_V \sin 2\theta_\Delta \cos(\phi_V + \phi_\Delta)$
R_{19}	$\text{Re}(\rho_{3,1}^{0,1} - \rho_{3,1}^{-1,0})$	$\frac{25}{32} \sqrt{6} \sin 2\theta_V \sin 2\theta_\Delta \cos(\phi_V - \phi_\Delta)$

^a Where $\rho_{n,n}^- = \rho_{n,n}^{1,1} + \rho_{n,n}^{-1,-1} - 2\rho_{n,n}^{0,0}$, and $\rho_{-}^{m,m'} = \rho_{3,3}^{m,m'} + \rho_{-3,-3}^{m,m'} - \rho_{1,1}^{m,m'} - \rho_{-1,-1}^{m,m'}$.

TABLE II. Joint decay correlations in $\pi^+ p \rightarrow \rho^0 \Delta^{++}$ at 3.7 GeV/c (θ -channel coordinate system).

Term	$r' [(GeV/c)^2]$										
	0.0-0.01	0.01-0.025	0.025-0.045	0.045-0.07	0.07-0.11	0.11-0.18	0.18-0.34	0.34-1.0	No. events		
	336	408	427	377	419	402	385	404			
R_1	0.868±0.041	0.861±0.038	0.765±0.036	0.769±0.038	0.766±0.038	0.723±0.036	0.611±0.040	0.161±0.033			
R_2	-0.001±0.027	-0.091±0.024	-0.074±0.025	-0.085±0.027	-0.086±0.024	-0.105±0.027	-0.077±0.025	-0.023±0.022			
R_3	0.045±0.026	-0.008±0.025	-0.015±0.025	-0.067±0.026	-0.009±0.025	-0.101±0.026	-0.045±0.029	-0.001±0.034			
R_4	0.084±0.032	0.072±0.028	0.100±0.029	0.116±0.030	0.150±0.029	0.148±0.030	0.193±0.030	0.259±0.028			
R_5	-0.001±0.031	-0.047±0.030	0.019±0.028	-0.043±0.030	-0.063±0.028	0.037±0.028	0.025±0.029	-0.064±0.026			
R_6	0.037±0.027	-0.019±0.024	0.024±0.025	-0.051±0.026	-0.027±0.025	-0.008±0.026	-0.008±0.027	0.111±0.027			
R_7	0.649±0.182	0.790±0.163	0.483±0.149	0.536±0.160	0.349±0.157	0.486±0.148	0.513±0.154	0.373±0.120			
U_7^a	0.532±0.112	0.564±0.097	0.388±0.081	0.351±0.084	0.259±0.077	0.238±0.073	0.095±0.051	0.009±0.029			
R_8	-0.023±0.065	-0.001±0.056	-0.042±0.057	0.004±0.060	0.072±0.056	0.005±0.060	0.079±0.063	-0.044±0.075			
U_8	-0.030±0.018	0.006±0.018	0.009±0.015	0.036±0.016	0.004±0.010	0.041±0.016	0.010±0.009	0.000±0.001			
R_9	-0.002±0.069	0.064±0.061	0.070±0.061	0.046±0.063	0.129±0.058	-0.002±0.069	0.027±0.060	-0.023±0.050			
U_9	0.001±0.018	0.065±0.020	0.044±0.017	0.046±0.018	0.034±0.014	0.043±0.017	0.018±0.011	-0.001±0.003			
R_{10}	-0.025±0.073	-0.062±0.065	-0.003±0.064	0.168±0.065	0.097±0.066	0.062±0.063	0.047±0.065	0.227±0.056			
U_{10}	-0.060±0.043	0.030±0.038	-0.032±0.032	0.067±0.034	0.035±0.032	0.009±0.030	0.007±0.022	0.058±0.018			
R_{11}	-0.063±0.084	0.063±0.081	-0.025±0.070	0.056±0.081	0.147±0.074	0.196±0.069	0.047±0.076	-0.138±0.056			
U_{11}	0.001±0.049	0.074±0.048	-0.024±0.036	0.057±0.040	0.082±0.037	0.043±0.033	-0.021±0.024	-0.033±0.015			
R_{12}	0.016±0.018	0.050±0.017	0.026±0.018	0.015±0.021	0.008±0.019	0.002±0.020	0.014±0.023	0.069±0.029			
U_{12}	0.002±0.002	0.000±0.001	0.000±0.001	0.003±0.002	0.000±0.001	0.001±0.003	0.000±0.001	0.000±0.004			
R_{13}	0.018±0.019	-0.004±0.018	0.005±0.019	-0.006±0.019	0.021±0.019	-0.041±0.021	0.008±0.024	0.055±0.028			
U_{13}	0.002±0.002	0.000±0.001	0.000±0.001	0.003±0.002	0.000±0.001	0.001±0.003	0.000±0.001	0.000±0.004			
R_{14}	-0.024±0.021	-0.036±0.020	0.005±0.020	-0.001±0.021	0.006±0.021	-0.017±0.021	-0.032±0.022	0.028±0.026			
U_{14}	0.000±0.001	0.000±0.001	0.000±0.001	0.003±0.002	0.001±0.002	0.004±0.003	-0.001±0.002	0.000±0.002			
R_{15}	-0.015±0.021	0.020±0.021	0.006±0.021	-0.015±0.021	0.018±0.021	-0.014±0.020	-0.037±0.023	0.026±0.025			
U_{15}	0.000±0.001	0.000±0.001	0.000±0.001	0.003±0.002	0.001±0.002	0.004±0.003	-0.001±0.002	0.000±0.002			
R_{16}	-0.011±0.038	-0.050±0.034	-0.104±0.034	-0.001±0.036	-0.034±0.036	-0.043±0.035	0.014±0.036	-0.099±0.034			
U_{16}	0.000±0.002	0.003±0.004	-0.004±0.004	0.008±0.005	0.004±0.004	0.002±0.005	0.001±0.004	-0.005±0.005			
R_{17}	-0.010±0.039	0.013±0.034	-0.057±0.035	0.001±0.039	0.041±0.036	-0.022±0.038	0.033±0.037	0.044±0.032			
U_{17}	0.000±0.002	0.003±0.004	-0.004±0.004	0.008±0.005	0.004±0.004	0.002±0.005	0.001±0.004	-0.005±0.005			
R_{18}	-0.106±0.044	-0.169±0.042	-0.176±0.040	-0.168±0.041	-0.099±0.039	-0.103±0.039	-0.149±0.039	-0.020±0.035			
U_{18}	0.000±0.000	0.009±0.006	-0.003±0.004	0.007±0.006	0.011±0.006	0.008±0.006	-0.004±0.005	0.003±0.003			
R_{19}	0.055±0.047	0.035±0.042	-0.073±0.040	0.024±0.044	0.087±0.038	0.011±0.039	0.018±0.041	-0.092±0.033			
U_{19}	0.000±0.000	0.009±0.006	-0.003±0.004	0.007±0.006	0.011±0.006	0.008±0.006	-0.004±0.005	0.003±0.003			

^a Here $U_7 = \frac{1}{2}(3\rho^{0,0} - 1)(1 - 4\rho_{3,3})$, $U_8 = (4\rho_{3,3} - 1)\rho^{1,-1}$, $U_9 = (4\rho_{3,3} - 1)\text{Re}\rho_{3,1}^{1,0}$, $U_{10} = (1 - 3\rho^{0,0})\text{Re}\rho_{3,1}^{1,0}$, $U_{11} = (1 - 3\rho^{0,0})\text{Re}\rho_{3,-1}$, $U_{12} = \rho^{1,-1}\text{Re}\rho_{3,-1}$, $U_{13} = \rho^{1,-1}\text{Re}\rho_{3,-1}$, $U_{14} = \rho^{1,-1}\text{Re}\rho_{3,1}^{1,0}$, $U_{15} = \rho^{1,-1}\text{Re}\rho_{3,1}^{1,0}$, $U_{16} = 2\text{Re}\rho_{3,1}^{1,0}$, $U_{17} = 2\text{Re}\rho_{3,-1}^{1,0}$, $U_{18} = 2\text{Re}\rho_{3,1}^{1,0}$, $U_{19} = 2\text{Re}\rho_{3,1}^{1,0}$.

TABLE III. Joint decay correlation in $\pi^+ p \rightarrow \omega^0 \Delta^{++}$ at 3.7 GeV/c (t -channel coordinate system). The symbols (U_N) are as defined in Table II.

Term	t' [(GeV/c) ²]			
	0.0-0.1	0.1-0.23	0.23-0.4	0.4-1.0
	350	No. events 396	392	388
R_1	0.540 ± 0.042	0.335 ± 0.038	0.382 ± 0.038	0.526 ± 0.041
R_2	-0.123 ± 0.024	-0.088 ± 0.022	-0.148 ± 0.023	-0.147 ± 0.022
R_3	-0.004 ± 0.030	0.052 ± 0.033	-0.017 ± 0.031	-0.038 ± 0.030
R_4	0.128 ± 0.031	0.208 ± 0.028	0.191 ± 0.029	0.161 ± 0.028
R_5	-0.045 ± 0.031	-0.053 ± 0.028	-0.041 ± 0.028	-0.038 ± 0.031
R_6	-0.008 ± 0.028	0.038 ± 0.025	0.016 ± 0.026	-0.023 ± 0.027
R_7	0.414 ± 0.150	0.514 ± 0.124	0.230 ± 0.136	0.442 ± 0.137
U_7	0.151 ± 0.049	0.001 ± 0.010	0.017 ± 0.016	0.103 ± 0.039
R_8	0.118 ± 0.068	0.025 ± 0.071	0.066 ± 0.070	0.081 ± 0.065
U_8	0.002 ± 0.015	-0.009 ± 0.008	0.004 ± 0.008	0.014 ± 0.011
R_9	0.049 ± 0.063	0.024 ± 0.051	0.120 ± 0.056	0.167 ± 0.056
U_9	0.060 ± 0.019	0.015 ± 0.011	0.035 ± 0.018	0.052 ± 0.019
R_{10}	0.065 ± 0.069	0.142 ± 0.053	0.011 ± 0.061	0.009 ± 0.062
U_{10}	0.005 ± 0.017	0.000 ± 0.004	-0.002 ± 0.004	0.014 ± 0.016
R_{11}	0.146 ± 0.079	0.057 ± 0.067	-0.013 ± 0.063	0.094 ± 0.076
U_{11}	0.028 ± 0.020	0.000 ± 0.006	0.006 ± 0.006	0.022 ± 0.018
R_{12}	0.092 ± 0.023	0.138 ± 0.027	0.140 ± 0.024	0.024 ± 0.024
U_{12}	0.000 ± 0.000	0.002 ± 0.002	0.000 ± 0.001	0.001 ± 0.001
R_{13}	-0.021 ± 0.024	0.023 ± 0.026	-0.041 ± 0.025	0.024 ± 0.024
U_{13}	0.000 ± 0.000	0.002 ± 0.002	0.000 ± 0.001	0.001 ± 0.001
R_{14}	-0.026 ± 0.026	0.069 ± 0.026	0.023 ± 0.026	-0.004 ± 0.023
U_{14}	0.000 ± 0.001	-0.003 ± 0.002	0.000 ± 0.001	0.001 ± 0.002
R_{15}	0.018 ± 0.025	0.003 ± 0.025	0.082 ± 0.025	0.011 ± 0.023
U_{15}	0.000 ± 0.001	-0.003 ± 0.002	0.000 ± 0.001	0.001 ± 0.002
R_{16}	0.036 ± 0.036	0.029 ± 0.034	0.081 ± 0.035	0.025 ± 0.035
U_{16}	0.002 ± 0.007	-0.007 ± 0.005	-0.005 ± 0.008	0.007 ± 0.008
R_{17}	0.011 ± 0.036	0.006 ± 0.034	0.022 ± 0.035	0.020 ± 0.034
U_{17}	0.002 ± 0.007	-0.007 ± 0.005	-0.005 ± 0.008	0.007 ± 0.008
R_{18}	-0.071 ± 0.043	-0.056 ± 0.040	-0.108 ± 0.039	-0.056 ± 0.040
U_{18}	0.011 ± 0.008	0.009 ± 0.006	0.012 ± 0.008	0.011 ± 0.009
R_{19}	0.038 ± 0.041	0.084 ± 0.039	0.053 ± 0.037	0.076 ± 0.039
U_{19}	0.011 ± 0.008	0.009 ± 0.006	0.012 ± 0.008	0.011 ± 0.009

background, typically, so that distortions of the density-matrix elements from this source are expected to be small. For the $\omega\Delta$ channel the background under the double-resonance events² is $\leq 10\%$ for t' as large as 0.3, so that background effects in this channel are expected to be negligible. As a check on the integrity of our data we have verified that the conditions⁹ imposed on the density matrices by the positivity requirement are satisfied.

III. INVESTIGATION OF CORRELATIONS

Donohue⁵ has pointed out that the expression of Pilkuhn and Svensson⁷ for the joint decay distribu-

tion may be reexpressed as the product of the well-known¹ single-vertex distributions for $J^P = 1^-$ (W_V) and $J^P = \frac{3}{2}^+$ (W_Δ), and an additional expression I that measures the correlation between the vector-meson and Δ^{++} decays:

$$W(\theta_V, \phi_V, \theta_\Delta, \phi_\Delta) = W_V(\theta_V, \phi_V) \times W_\Delta(\theta_\Delta, \phi_\Delta) + I(\theta_V, \phi_V, \theta_\Delta, \phi_\Delta). \quad (5)$$

Using the method of moments we have determined the t -channel joint decay density-matrix elements from the orthogonal expansion of Pilkuhn and Svensson. Table I shows the normalization adopted for the measured terms. In Tables II and III we present our data for channels (3) and (4),

respectively (in these tables, as well as in other results quoted below, the errors assigned are statistical only). Following Donohue,⁵ we also present the products of single-vertex density-matrix elements which contribute to the specified angular functions.¹⁰ The resulting differences ($D_i = R_i - U_i$), whose departure from zero signifies the presence of correlated decays, are plotted in Figs. 1 and 2 as functions of t' . With the exception of element R_7 , the product of single vertex elements is a small quantity with small errors (relative to the joint decay term); therefore these figures may also be viewed as illustrating the t' dependence of the joint decay matrix elements R_8 through R_{19} .

It may be seen that most of the correlation terms do not differ significantly from zero for either $\rho^0\Delta^{++}$ or $\omega\Delta^{++}$. Systematic departures from zero as a function of t' may be seen for the elements

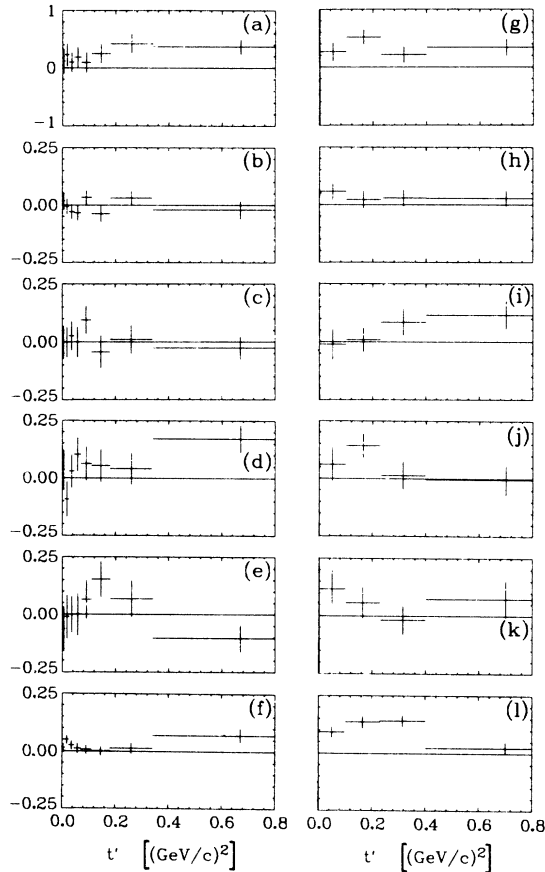


FIG. 1. $\rho\Delta$ and $\omega\Delta$ joint decay correlation terms 7–12. For $\rho\Delta$: (a) D_7 , (b) D_8 , (c) D_9 , (d) D_{10} , (e) D_{11} , (f) D_{12} . For $\omega\Delta$: (g) D_7 , (h) D_8 , (i) D_9 , (j) D_{10} , (k) D_{11} , (l) D_{12} .

$$D_7 \propto (1 - 3 \cos^2 \theta_\nu)(1 - 3 \cos^2 \theta_\Delta) \quad (6)$$

for both $\rho^0\Delta^{++}$ [Fig. 1(a)] and $\omega\Delta^{++}$ [Fig. 1(g)],

$$D_{12} \propto \sin^2 \theta_\nu \sin^2 \theta_\Delta \cos 2(\phi_\nu + \phi_\Delta) \quad (7)$$

for $\omega\Delta^{++}$ [Fig. 1(l)],

$$D_{18} \propto \sin 2\theta_\nu \sin 2\theta_\Delta \cos(\phi_\nu + \phi_\Delta) \quad (8)$$

for both $\rho^0\Delta^{++}$ [Fig. 2(f)] and $\omega\Delta^{++}$ [Fig. 2(m)], and

$$D_{19} \propto \sin 2\theta_\nu \sin 2\theta_\Delta \cos(\phi_\nu - \phi_\Delta) \quad (9)$$

for $\omega\Delta^{++}$ [Fig. 2(n)].

We note that the dominant correlations, D_7 , D_{12} , and D_{18} , are precisely those terms which are

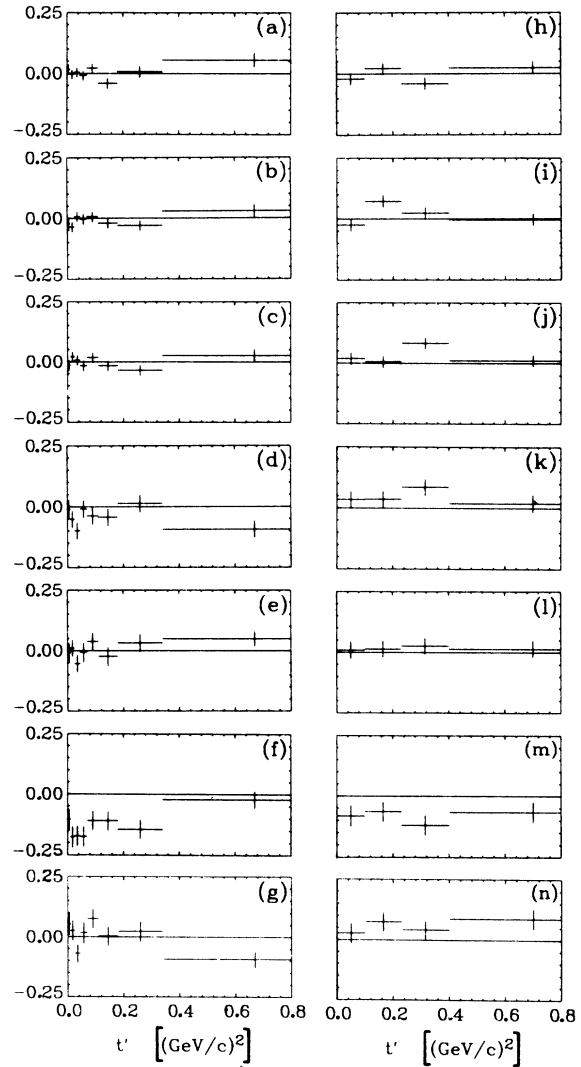


FIG. 2. $\rho\Delta$ and $\omega\Delta$ joint decay correlation terms 13–19. For $\rho\Delta$: (a) D_{13} , (b) D_{14} , (c) D_{15} , (d) D_{16} , (e) D_{17} , (f) D_{18} , (g) D_{19} . For $\omega\Delta$: (h) D_{13} , (i) D_{14} , (j) D_{15} , (k) D_{16} , (l) D_{17} , (m) D_{18} , (n) D_{19} .

TABLE IV. Joint decay density-matrix elements for $\rho^0\Delta^{++}$ at 3.7 GeV/c (s -channel coordinate system).

Term	$t'[(\text{GeV}/c)^2]$							
	0.000–0.010	0.010–0.025	0.025–0.045	0.045–0.070	0.07–0.11	0.11–0.18	0.18–0.34	0.34–1.00
R_1	0.844 ± 0.041	0.853 ± 0.040	0.707 ± 0.039	0.683 ± 0.043	0.588 ± 0.038	0.547 ± 0.042	0.394 ± 0.040	0.394 ± 0.037
R_2	0.098 ± 0.027	0.107 ± 0.023	0.148 ± 0.022	0.175 ± 0.024	0.219 ± 0.022	0.194 ± 0.023	0.137 ± 0.024	0.045 ± 0.022
R_3	0.032 ± 0.027	-0.012 ± 0.025	-0.044 ± 0.026	-0.110 ± 0.026	-0.098 ± 0.027	-0.189 ± 0.028	-0.154 ± 0.032	0.116 ± 0.031
R_4	0.097 ± 0.032	0.079 ± 0.029	0.190 ± 0.028	0.146 ± 0.029	0.169 ± 0.028	0.220 ± 0.027	0.283 ± 0.028	0.352 ± 0.026
R_5	0.071 ± 0.031	0.076 ± 0.029	0.139 ± 0.027	0.087 ± 0.030	0.080 ± 0.029	0.093 ± 0.029	0.010 ± 0.029	0.061 ± 0.026
R_6	0.030 ± 0.027	-0.023 ± 0.024	-0.027 ± 0.026	-0.069 ± 0.026	-0.038 ± 0.025	-0.050 ± 0.027	-0.060 ± 0.029	0.058 ± 0.030
R_7	0.524 ± 0.178	0.484 ± 0.172	-0.223 ± 0.150	-0.031 ± 0.155	0.191 ± 0.136	-0.271 ± 0.137	-0.141 ± 0.125	0.186 ± 0.112
R_8	-0.020 ± 0.068	0.047 ± 0.060	0.160 ± 0.063	0.127 ± 0.061	0.149 ± 0.064	0.102 ± 0.065	-0.054 ± 0.074	0.248 ± 0.069
R_9	-0.106 ± 0.067	-0.200 ± 0.057	-0.176 ± 0.052	-0.176 ± 0.059	-0.115 ± 0.056	-0.112 ± 0.053	0.030 ± 0.051	0.065 ± 0.048
R_{10}	-0.007 ± 0.073	0.007 ± 0.070	0.053 ± 0.072	0.193 ± 0.073	0.136 ± 0.063	0.014 ± 0.069	0.097 ± 0.069	-0.035 ± 0.065
R_{11}	-0.202 ± 0.083	-0.294 ± 0.079	-0.326 ± 0.073	-0.131 ± 0.082	-0.160 ± 0.072	-0.008 ± 0.075	0.175 ± 0.071	-0.146 ± 0.060
R_{12}	0.021 ± 0.019	0.050 ± 0.017	0.017 ± 0.019	-0.012 ± 0.020	-0.018 ± 0.022	-0.006 ± 0.022	0.001 ± 0.025	0.098 ± 0.025
R_{13}	0.018 ± 0.019	-0.012 ± 0.017	0.004 ± 0.019	0.033 ± 0.021	0.027 ± 0.021	0.027 ± 0.022	0.105 ± 0.025	0.047 ± 0.026
R_{14}	-0.005 ± 0.021	0.027 ± 0.020	0.059 ± 0.021	0.041 ± 0.024	0.035 ± 0.022	-0.012 ± 0.025	-0.013 ± 0.025	0.047 ± 0.022
R_{15}	-0.010 ± 0.021	0.004 ± 0.021	0.013 ± 0.022	-0.041 ± 0.023	-0.043 ± 0.023	-0.080 ± 0.025	-0.060 ± 0.026	-0.036 ± 0.023
R_{16}	0.015 ± 0.039	0.056 ± 0.034	-0.005 ± 0.035	0.005 ± 0.037	0.016 ± 0.035	0.005 ± 0.035	-0.040 ± 0.037	0.017 ± 0.037
R_{17}	-0.006 ± 0.040	-0.002 ± 0.034	-0.029 ± 0.035	-0.107 ± 0.035	-0.054 ± 0.036	-0.074 ± 0.035	-0.089 ± 0.037	0.035 ± 0.038
R_{18}	-0.090 ± 0.044	-0.110 ± 0.040	-0.038 ± 0.037	-0.010 ± 0.041	-0.040 ± 0.039	0.075 ± 0.037	-0.000 ± 0.038	-0.011 ± 0.037
R_{19}	0.082 ± 0.047	0.105 ± 0.039	0.054 ± 0.036	0.087 ± 0.039	0.103 ± 0.039	0.075 ± 0.037	0.008 ± 0.040	-0.036 ± 0.038

allowed⁵ to be nonvanishing at 0° by angular momentum conservation. Other experiments^{3, 4, 11} studying vector-meson- Δ^{++} production have observed similar effects with data averaged over a single t' bin. The original observation of correlation effects by Goldhaber *et al.*³ relates to the D_7 term, which gives a $\cos\theta_V\text{-}\cos\theta_\Delta$ correlation. To the best of our knowledge this is the first time this correlation has been observed for $\omega\Delta^{++}$ as

well. Previous experiments have noted its presence in $\rho^0\Delta^{++}$ (Refs. 3, 4) and $K^*\Delta^{++}$ reactions.¹¹

For completeness in presenting the data, we include the joint decay density-matrix elements evaluated in the s -channel coordinate systems. These frames are defined in the text and coincide with the corresponding t -channel frames for $t'=0$. In Table IV are presented our $\rho^0\Delta^{++}$ data, and in Table V our $\omega\Delta^{++}$ data.

TABLE V. Joint decay density-matrix elements for $\omega\Delta^{++}$ at 3.7 GeV/c (s -channel coordinate system).

Term	$t'[(\text{GeV}/c)^2]$			
	0.0–0.1	0.1–0.23	0.23–0.40	0.40–1.0
R_1	0.613 ± 0.041	0.414 ± 0.039	0.446 ± 0.039	0.266 ± 0.037
R_2	0.030 ± 0.025	0.055 ± 0.022	0.128 ± 0.022	0.122 ± 0.023
R_3	0.032 ± 0.031	0.091 ± 0.032	0.015 ± 0.031	-0.168 ± 0.033
R_4	0.144 ± 0.032	0.257 ± 0.028	0.269 ± 0.028	0.265 ± 0.028
R_5	0.097 ± 0.030	0.079 ± 0.027	0.070 ± 0.027	0.031 ± 0.030
R_6	-0.017 ± 0.028	0.010 ± 0.028	-0.030 ± 0.028	-0.083 ± 0.028
R_7	0.403 ± 0.167	0.396 ± 0.135	0.302 ± 0.131	0.206 ± 0.126
R_8	0.176 ± 0.072	0.248 ± 0.064	0.084 ± 0.066	-0.102 ± 0.068
R_9	-0.130 ± 0.062	0.025 ± 0.052	0.044 ± 0.053	-0.005 ± 0.054
R_{10}	0.102 ± 0.061	0.094 ± 0.066	0.135 ± 0.061	-0.018 ± 0.064
R_{11}	-0.106 ± 0.074	-0.004 ± 0.065	-0.087 ± 0.068	-0.017 ± 0.064
R_{12}	0.046 ± 0.022	0.023 ± 0.027	-0.019 ± 0.026	0.021 ± 0.027
R_{13}	-0.003 ± 0.024	0.101 ± 0.025	0.064 ± 0.026	0.112 ± 0.027
R_{14}	0.021 ± 0.025	0.026 ± 0.024	-0.018 ± 0.024	-0.009 ± 0.026
R_{15}	-0.026 ± 0.024	-0.065 ± 0.025	-0.050 ± 0.024	-0.014 ± 0.027
R_{16}	0.104 ± 0.039	-0.025 ± 0.036	0.012 ± 0.038	-0.045 ± 0.035
R_{17}	-0.044 ± 0.040	-0.081 ± 0.035	-0.173 ± 0.037	-0.079 ± 0.034
R_{18}	0.008 ± 0.042	0.129 ± 0.037	0.100 ± 0.037	0.003 ± 0.037
R_{19}	0.023 ± 0.040	-0.000 ± 0.038	-0.120 ± 0.038	0.008 ± 0.036

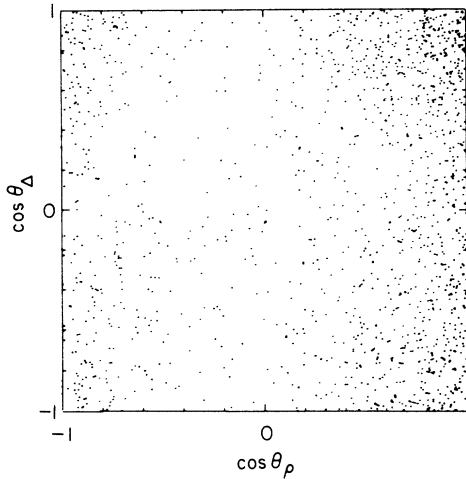


FIG. 3. Correlation plot of $\cos\theta_\rho$ vs $\cos\theta_\Delta$ for $\rho\Delta$ events with $t' < 0.07$ (GeV/c)² (1548 events).

IV. VISUALIZATION OF CORRELATIONS

The previous section demonstrated the existence of various correlation terms relating the vector-meson decays to the Δ^{++} decays by evaluating moments of the decay angular distribution. A more direct and intuitively appealing demonstration is to display the breakdown of factorization inherent in Eq. (5). This can be done by exhibiting changes in the distributions in one set of variables when cuts are performed on another set of variables. This was the procedure followed originally³ in establishing a $\cos\theta_\nu$ - $\cos\theta_\Delta$ correlation in the $\rho^0\Delta^{++}$ channel. In Fig. 3 we show a plot of our $\rho^0\Delta^{++}$ data with $t' < 0.07$ (GeV/c)², plotting $\cos\theta_\rho$ vs $\cos\theta_\Delta$. It may be seen that the distribution of $\cos\theta_\Delta$ peaks near ± 1 for polar ρ decays ($|\cos\theta_\rho| \approx 1$), and is more uniform for equatorial ρ decays ($\cos\theta_\rho \approx 0$).

The projections on the $\cos\theta_\rho$ and $\cos\theta_\Delta$ axes for polar ($|\cos\theta| > 0.4$) and equatorial ($|\cos\theta| < 0.4$) cuts on the decay angles of the other decaying system are shown in Fig. 4. The ρ^0 data are folded about $\cos\theta_\rho = 0$ to eliminate, to first order, the effects of the ϵ . The curves in this figure are calculated from the observed values of R_1 , R_4 , and R_7 of Table II, taking into account the angular cuts performed on the data. The correlation effect is evident from a comparison of Figs. 4(b) and 4(d), the $\cos\theta_\Delta$ distributions for polar and equatorial ρ^0 decays, respectively.

The s -wave $\pi^+\pi^-$ amplitude in the vicinity of the ρ^0 mass leads to the strong forward-backward decay asymmetry of the ρ^0 in Fig. 3. However, the agreement of the four experimental distributions of Fig. 4 in both magnitude and shape with the curves calculated assuming a pure $J^P = 1^- \pi^+\pi^-$

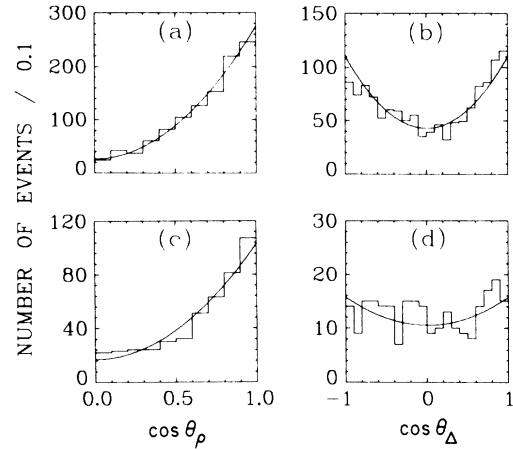


FIG. 4. Projections of the $\cos\theta_\rho$ - $\cos\theta_\Delta$ plot for $\rho\Delta$ events with $t' < 0.07$ (GeV/c)² (1548 events) for polar and equatorial cuts. (a) $|\cos\theta_\Delta| > 0.4$ (1091 events), (b) $|\cos\theta_\rho| > 0.4$ (1292 events), (c) $|\cos\theta_\Delta| < 0.4$ (457 events), (d) $|\cos\theta_\rho| < 0.4$ (256 events).

state (as well as a pure $J^P = \frac{3}{2}^+ p\pi^+$) by means of only one over-all normalization to the total number of events suggests that the ϵ does not severely distort the observed density-matrix elements. We shall return to this point when discussing the correlation D_{18} .

A similar correlation effect is present in the $\omega\Delta^{++}$ channel, and, as evidenced by a comparison of Figs. 1(a) and 1(g), this correlation is even larger than for $\rho^0\Delta^{++}$. The plot of $\cos\theta_\omega$ vs $\cos\theta_\Delta$ is shown in Fig. 5, and the polar and equatorial projections in Fig. 6. In this case the correlation is clearly displayed in both the $\cos\theta_\omega$ and the $\cos\theta_\Delta$ distributions. The curves on Fig. 6, which were calculated in a manner similar to those for Fig. 4, are again in agreement with the data, both in magnitude and shape.

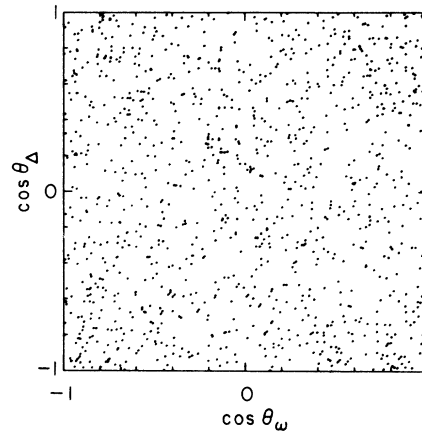


FIG. 5. Correlation plot of $\cos\theta_\omega$ vs $\cos\theta_\Delta$ for $\omega\Delta$ events with $t' < 0.4$ (GeV/c)² (1138 events).

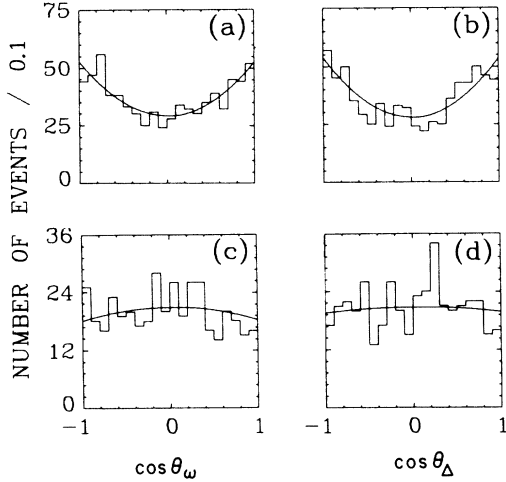


FIG. 6. Projections of the $\cos\theta_\omega$ - $\cos\theta_\Delta$ plot for $\omega\Delta$ events with $t' < 0.4$ (GeV/c)² (1138 events) for polar and equatorial cuts. (a) $|\cos\theta_\Delta| > 0.4$ (738 events), (b) $|\cos\theta_\omega| > 0.4$ (723 events), (c) $|\cos\theta_\Delta| < 0.4$ (400 events), (d) $|\cos\theta_\omega| < 0.4$ (415 events).

We next consider the correlation term D_{12} , which is clear for the $\omega\Delta$ channel [Fig. 1(l)] but probably not significant for the $\rho\Delta$ channel [Fig. 1(f)]. For visualization purposes we therefore consider only the $\omega\Delta$ data. To enhance the appearance of this term we use the functional form of Eq. (7), and select $\omega\Delta$ events [with $t' < 0.4$ (GeV/c)²] with large values of $\sin^2\theta$:

$$0 < |\cos\theta_\omega| < 0.5, \quad (10a)$$

$$0 < |\cos\theta_\Delta| < 0.5. \quad (10b)$$

The selected data are plotted on Fig. 7 in the form

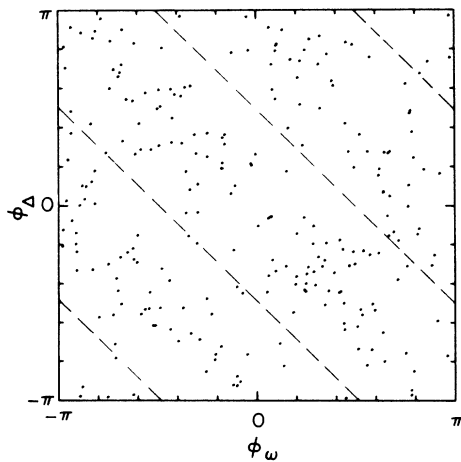


FIG. 7. Correlation plot of ϕ_ω vs ϕ_Δ for $\omega\Delta$ events with $t' < 0.4$ (GeV/c)² and $|\cos\theta_\omega| < 0.5$, $|\cos\theta_\Delta| < 0.5$ (253 events).

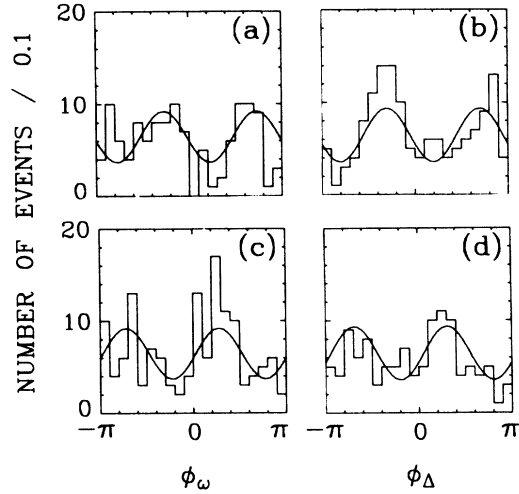


FIG. 8. Projections of the ϕ_ω -vs- ϕ_Δ correlation plot (Fig. 7). (a) $0 < \phi_\Delta < \frac{1}{2}\pi$ or $-\pi < \phi_\Delta < -\frac{1}{2}\pi$ (118 events), (b) $0 < \phi_\omega < \frac{1}{2}\pi$ or $-\pi < \phi_\omega < -\frac{1}{2}\pi$ (139 events), (c) $\frac{1}{2}\pi < \phi_\Delta < \pi$ or $-\frac{1}{2}\pi < \phi_\Delta < 0$ (135 events), and (d) $\frac{1}{2}\pi < \phi_\omega < \pi$ or $-\frac{1}{2}\pi < \phi_\omega < 0$ (114 events).

of a plot of ϕ_ω vs ϕ_Δ , with dashed lines selected to lie along the values

$$\cos 2(\phi_\omega + \phi_\Delta) = 0.$$

The data are seen to display valleys centered on these lines.

The projections of Fig. 7 onto the ϕ_ω and ϕ_Δ axes are shown in Fig. 8 (as for D_7 we display the V^0 variable with different decay angle cuts for the Δ^{++} , and vice versa). The presence of a $\phi_\omega - \phi_\Delta$ correlation is evident from a comparison either of Fig. 8(a) with 8(c), or of Fig. 8(b) with 8(d). We also see in these projections evidence for a period of π , in agreement with the expected functional ϕ dependence.

The remaining correlation term that we shall illustrate is D_{18} . This term's contribution vanishes if any of the decay angles are integrated over. A display of such a term therefore cannot be as straightforward as the other terms considered. To avoid cancellation of the effect we consider two separate plots of ϕ_ν vs ϕ_Δ ; one is chosen to contain those events with $(\sin 2\theta_\nu \sin 2\theta_\Delta) > 0$, and the other $(\sin 2\theta_\nu \sin 2\theta_\Delta) < 0$. Binning these plots and subtracting the contents of the one with a negative value of $\sin 2\theta_\nu \sin 2\theta_\Delta$ from that of the positive one, we present in Fig. 9 a subtracted plot table of ϕ_ρ vs ϕ_Δ for $\rho^0\Delta^{++}$ events with $t' < 0.07$ (GeV/c)².

The sign pattern on the ϕ_ρ -vs- ϕ_Δ plot suggested by the ϕ dependence of Eq. (8) is clearly evident in Fig. 9. In Fig. 10 we show the projections of this plot, illustrating the changes in shape of the distribution of ϕ_ρ (ϕ_Δ) when different cuts are

made on ϕ_Δ (ϕ_ρ). The period of the data is seen to be 2π , as expected from Eq. (8). The experimental subtracted distributions in Figs. 9 and 10 do not average to zero when integrated over all angles due to the asymmetries resulting from the ρ interference with the ϵ (and to a lesser extent the Δ interference with background). Comparison of the curves obtained from the measured density-matrix elements with the subtracted data indicates that the value of the relevant joint density-matrix element is probably not affected to first order by the interference.

Similar displays for $\omega\Delta$ are not as statistically significant as for $\rho\Delta$; with more data one should be able to visualize both D_{18} and D_{19} for $\omega\Delta$.

V. $\rho^0\Delta^{**}$ AND $\omega\Delta^{**}$ PRODUCTION AMPLITUDES AT 0°

The constraints of angular momentum conservation at 0° production angle lead⁵ to the vanishing of most of the density-matrix elements of Table I. With the choice of independent nonvanishing helicity amplitudes $f_{\lambda_V, 2\lambda_\Delta; 2\lambda_N}$ (at 0° these amplitudes will be identical for s - and t -channel axes) as

$$A_0 = f_{0,1;1} \quad ,$$

$$A_3 = f_{1,3;1} \quad ,$$

$$A_1 = f_{1,1;-1} \quad ,$$

one finds⁵

$$R_1 = \rho^{0,0} = \frac{2}{N} |A_0|^2 \quad ,$$

$$R_4 = \rho_{3,3} = \frac{1}{N} |A_3|^2 \quad ,$$

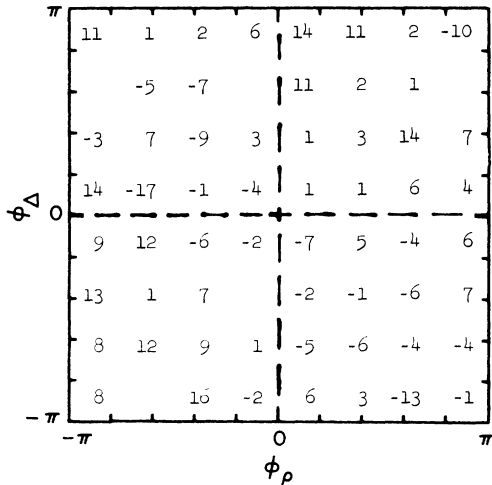


FIG. 9. Subtracted correlation plot of ϕ_ρ vs ϕ_Δ for $\rho\Delta$ events with $t' < 0.07$ (GeV/c)². See text for details of the subtraction procedure.

$$R_{12} = \rho_{3,-1}^{1,-1} = \frac{1}{N} \text{Re}(A_3 A_1^*) \quad ,$$

$$R_{18} = \rho_{3,1}^{1,0} = \frac{1}{N} \text{Re}(A_3 A_0^*) \quad ,$$

while all other terms must vanish at 0° . The trace condition which these amplitudes must satisfy is written as

$$2(|A_0|^2 + |A_3|^2 + |A_1|^2) = N \quad .$$

Using this condition

$$\left| \frac{A_3}{A_0} \right|^2 = \frac{2\rho_{3,3}}{\rho^{0,0}} \quad ,$$

$$\left| \frac{A_1}{A_3} \right|^2 = \frac{1 - \rho^{0,0} - 2\rho_{3,3}}{2\rho_{3,3}} \quad ,$$

$$\cos(\phi_3 - \phi_0) = \frac{\rho_{3,1}^{1,0}}{(\frac{1}{2}\rho_{3,3}\rho^{0,0})^{1/2}} \quad ,$$

and

$$\cos(\phi_3 - \phi_1) = \frac{\rho_{3,-1}^{1,-1}}{[\frac{1}{2}\rho_{3,3}(1 - \rho^{0,0} - 2\rho_{3,3})]^{1/2}} \quad ,$$

where ϕ_0 is the phase of A_0 , ϕ_3 that of A_3 , and ϕ_1 that of A_1 .

In Table VI we summarize our experimental results for the $\rho\Delta$ [$t' < 0.07$ (GeV/c)²], and $\omega\Delta$ [$t' < 0.1$ (GeV/c)²] channels. The momentum-transfer intervals are chosen such that the maximum helicity crossing angle is $\leq 45^\circ$, and also so that enough events are included to allow a meaningful determination. Ideally, of course, one would

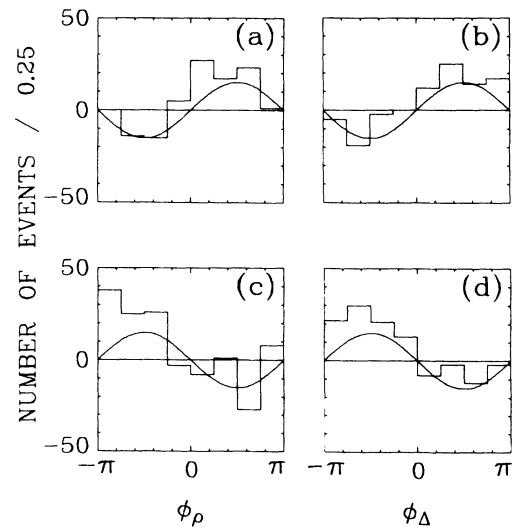


FIG. 10. Projections of the subtracted ϕ_ρ -vs- ϕ_Δ correlation plot (Fig. 9). (a) $0 < \phi_\Delta < \pi$, (b) $0 < \phi_\rho < \pi$, (c) $-\pi < \phi_\Delta < 0$, and (d) $-\pi < \phi_\rho < 0$.

choose as narrow a t' interval as practical to eliminate possible biases from amplitudes which may deviate from zero values as the production angle increases from 0° .

The results of Table VI are consistent with a simple model motivated by Regge theory. If a single trajectory contributes to an amplitude A_i , the phase of A_i is given by the signature factor

$$\frac{1 + \tau e^{-i\pi\alpha}}{\sin\pi\alpha},$$

where $\tau = (-1)^J$ for the exchange of a particle of spin J on trajectory α . The dominant exchanges² for $\pi p \rightarrow \rho \Delta$ are expected to be π (unnatural parity) and A_2 (natural parity), while for $\omega \Delta$ they are B (unnatural parity) and ρ (natural parity). Exchange degeneracy leads to the relations

$$\begin{aligned}\alpha_\pi &= \alpha_B \simeq t, \\ \alpha_\rho &= \alpha_{A_2} \simeq t + 0.5.\end{aligned}$$

Therefore at small t the phases of the contributing trajectories are

$$\begin{aligned}\phi_\pi &= 0 = \phi_B - \frac{1}{2}\pi, \\ \phi_{A_2} &= -\frac{1}{4}\pi = \phi_\rho - \frac{1}{2}\pi.\end{aligned}$$

We note that only unnatural-parity-exchange amplitudes can contribute¹ to A_0 . If we assume that A_1 and A_3 are dominated by a single evasive natural-parity amplitude, we are led to the identification

$$\phi_3 - \phi_0 = \begin{cases} \phi_{A_2} - \phi_\pi + k\pi & \text{for } \rho\Delta \\ \phi_\rho - \phi_B + k\pi & \text{for } \omega\Delta \end{cases}$$

as well as the relation

$$\phi_3 - \phi_1 = 0.$$

Here $k=0$ or 1 allows for the presence of a possible over-all minus sign of the relative π - A_2 amplitudes arising from the reduced residues. This model thus predicts that

TABLE VI. Summary of $\rho^0 \Delta^{++}$ and $\omega \Delta^{++}$ data near 0° .

	$\rho^0 \Delta^{++}$ [$t' < 0.07$ (GeV/c) ²]	$\omega \Delta^{++}$ [$t' < 0.10$ (GeV/c) ²]
$\rho^{0,0}$	0.814 ± 0.019	0.540 ± 0.042
$\rho_{3,3}$	0.093 ± 0.015	0.128 ± 0.031
$\rho_{3,1}^{1,-1}$	0.027 ± 0.009	0.092 ± 0.023
$\rho_{3,1}^{1,0}$	-0.157 ± 0.021	-0.071 ± 0.043
$ A_3/A_0 ^2$	0.228 ± 0.036	0.48 ± 0.12
$ A_1/A_3 ^2$	0.0 ± 0.2	0.80 ± 0.45
$\cos(\phi_3 - \phi_0)$	-0.81 ± 0.13	-0.38 ± 0.24
$\cos(\phi_3 - \phi_1)$...	0.81 ± 0.22

$$\cos(\phi_3 - \phi_0) = \frac{(-1)^k}{\sqrt{2}}$$

for both $\rho\Delta$ and $\omega\Delta$. The data are seen to be consistent with this result for both reactions with $k=1$. It is also seen that the relative phase $\phi_3 - \phi_1$ for $\omega\Delta$ agrees with this model; for $\rho\Delta$ the data are not adequate to determine this number.

In principle the magnitudes of the amplitudes could serve as further checks on theoretical models. For our data sample, however, the statistical errors appear too large to allow definite conclusions to be drawn.

The joint decay correlations have thus been shown to yield definitive information about production amplitudes. A more complete analysis of the extraction of amplitudes from the measured joint decay density matrix will be published separately.¹² In another paper⁶ we will present a comparison of these data with the predictions of the nonrelativistic quark model.

ACKNOWLEDGMENTS

We wish to acknowledge the many contributions of Dr. Donald Coyne to earlier phases of this experiment. We further thank our scanners and measurers, the Data Handling staff under Howard White, and the Special Projects Group under Jack Franck for their cooperation.

*Work supported by the U. S. Atomic Energy Commission.

†Present address: Department of Physics, Imperial College, London, England.

‡Present address: Department of Physics, David Lipscomb College, Nashville, Tennessee 37203.

§On sabbatical leave from University of California, Berkeley; Guggenheim Fellow at CERN.

||Present address: Fysich Laboratorium, Toernooiveld, Nijmegen, The Netherlands.

¹K. Gottfried and J. D. Jackson, *Nuovo Cimento* **33**, 309 (1964).

²G. S. Abrams, K. W. J. Barnham, W. R. Butler, D. G. Coyne, G. Goldhaber, B. H. Hall, and J. MacNaughton, *Phys. Rev. Letters* **25**, 617 (1970); LBL Internal Memo UCID-3488, 1970 (unpublished).

³G. Goldhaber, J. L. Brown, I. Butterworth, S. Goldhaber, A. A. Hirata, J. A. Kadyk, B. C. Shen, and G. H. Trilling, *Phys. Letters* **18**, 76 (1965).

⁴K. Böckmann *et al.* (Bonn-Durham-Nijmegen-Paris-Strasbourg-Turin Collaboration), *Nucl. Phys.* **B7**, 681 (1968).

⁵J. T. Donohue, *Nuovo Cimento* **52A**, 1152 (1967).

⁶G. S. Abrams and K. W. J. Barnham, following paper,

Phys. Rev. D 7, 1395 (1973).

⁷H. Pilkuhn and B. E. Y. Svensson, *Nuovo Cimento* 38, 518 (1965), with the terms involving $\sin 2\theta_\alpha$ in Eq. (37h) multiplied by a further factor $1/\sqrt{2}$.

⁸A. Kotanski and K. Zalewski, *Nucl. Phys.* B22, 317 (1970).

⁹J. Daboul, *Nucl. Phys.* B4, 180 (1967).

¹⁰A more complete description of the general decay angular distribution written as a product term plus a correlation expression may be found in the invited paper of K. W. J. Barnham, in *Proceedings of the Seventh*

Rencontre de Moriond, edited by J. Tran Thanh Van (CNRS, Paris, 1972), Vol. I.

¹¹W. DeBaere *et al.* (Bruxelles-CERN Collaboration), *Nuovo Cimento* 61A, 397 (1969); B. Haber *et al.* (S.A.B.R.E. Collaboration), *Nucl. Phys.* B17, 289 (1970); G. S. Abrams, L. Eisenstein, J. Kim, D. Marshall, T. A. O'Halloran, Jr., W. Shufeldt, and J. Whitmore, *Phys. Rev. D* 1, 2433 (1970).

¹²G. S. Abrams, K. W. J. Barnham, and J. J. Bisognano (unpublished).